Diffusion of Microspheres in Sealed and Open Microarrays

B. RIEGER,[1]* H.R.C. DIETRICH,[2] L.R. VAN DEN DOEL,[3] AND L.J. VAN VLIET[2]
[1]*Department of Molecular Biology, Max-Planck-Institute for Biophysical Chemistry, Am Faßberg 11, 37077 Göttingen, Germany*
[2]*Quantitative Imaging Group, Faculty of Applied Sciences, Delft University of Technology, Lorentzweg 1, 2628 CJ Delft, The Netherlands*
[3]*Roosevelt Academy, Lange Noordstraat 1, 4330 AB Middelburg, The Netherlands*

KEY WORDS Brownian motion; diffusion; mean square displacement; microarrays; microbeads

ABSTRACT In several experiments, we study the diffusion of microspheres with different radii in microarrays filled with a variety of aqueous solutions of ethylene glycol. We study diffusion in open and closed (sealed) microarrays. In sealed nanoliter wells, the tracers show pure diffusion, whereas in open reactors, a radial outward-directed evaporation-induced liquid flow is superimposed onto the diffusion. In general, one of the following quantities can be calculated if the others are known: the temperature, the viscosity of the medium, the radius of the microbeads, or the diffusion constant. The estimated diffusion constants in closed microarrays are in good agreement with theoretical predictions based on the Brownian motion. We monitor the motion of the microbeads under a microscope and extract their paths in time from the digital recordings. Ambiguous paths due to the crossing of two trajectories can be detected. We show that low microsphere concentrations or high viscosities do not hamper a robust estimation of the diffusion parameters. *Microsc. Res. Tech. 65:218–225, 2004.*

INTRODUCTION

The characterization of the mobility of tracer molecules is an important issue in molecular cell biology, e.g., the diffusion of membrane proteins provides important information about membrane structure and interactions between membrane parts. The diffusion constant is one important feature to characterize mobility. One way to estimate the diffusion constant in living cells is Fluorescence Recovery After Photobleaching (FRAP) (Axelrod et al., 1976; Sprague et al., 2004). Here, after photobleaching of a small region, the recovery of the intensity in that region due to diffusion from the surroundings is monitored. Another way to measure diffusion is by is single particle tracking (Kubitscheck et al., 2000). This method does not only allow for measuring the diffusion constant, but also for characterizing the motion from Mean Square Displacement (MSD) graphs (Qian et al., 1991) if one particle can be traced over a sufficiently long time or from jump histograms (Kues and Kubitscheck, 2002) if a sufficiently large number of molecules is observed for a short amount of time.

Up to now, most work has been directed towards the accuracy and precision of the estimated diffusion constant as measured by particle tracking (Kutsumi et al., 1993; Qian et al., 1991; Saxton, 1997). Their work was solely based on simulations of the diffusion equation, possibly including binding effects. Based on the performance in simulation experiments, conclusions were drawn w.r.t. relevant biological questions. We investigate experimentally the process of estimating the diffusion constant and compare the results with a known ground truth obtained from the relation of the diffusion constant with three other parameters: the viscosity of the medium, the radius of the tracer, and the temperature. We also analyze the influence of the location estimation of each tracer per time point on the systematic error of the diffusion constant.

Proteins are probes of a size comparable to the surrounding molecules in the cell. This makes it unreliable to compute their diffusion constant from the abovementioned three parameters, as there is no satisfactory relation between diffusion and the bulk viscosity for these probes (Valeur, 2002). Therefore, we study in several experiments the diffusion of microspheres with radii in the order of 50–1,000 nm in the nanoliter wells of micromachined microarrays (Dietrich et al., 2004; Young et al., 2003). A variety of aqueous solutions of ethylene glycol is used as a medium. We perform the experiments in open and sealed wells. The sealing is achieved by a glass cover slip to prevent evaporation. This ensures that the liquid is stationary for these cases, as evaporation in (circular) microwells leads to an outward-directed radial flow (Doel and Vliet, 2001; Rieger et al., 2003). However, we also investigate the diffusion in the open wells to study the changes in the MSD graphs and to study the influence of a liquid flow on the diffusion constant estimation.

Via the Einstein relation (Einstein, 1905), one of the following quantities can be calculated if the others are known: the temperature T, the viscosity of the medium η, the radius of the microbeads r, or the diffusion constant D

*Correspondence to: Bernd Rieger, Department of Molecular Biology, Max-Planck-Institute for Biophysical Chemistry, Am Faßberg 11, 37077 Göttingen, Germany. E-mail: brieger@gwdg.de

Received 11 November 2004; accepted 18 November 2004

Contract grant sponsor: Netherlands Organization for Scientific Research (NWO).

DOI 10.1002/jemt.20128

Published online in Wiley InterScience (www.interscience.wiley.com).

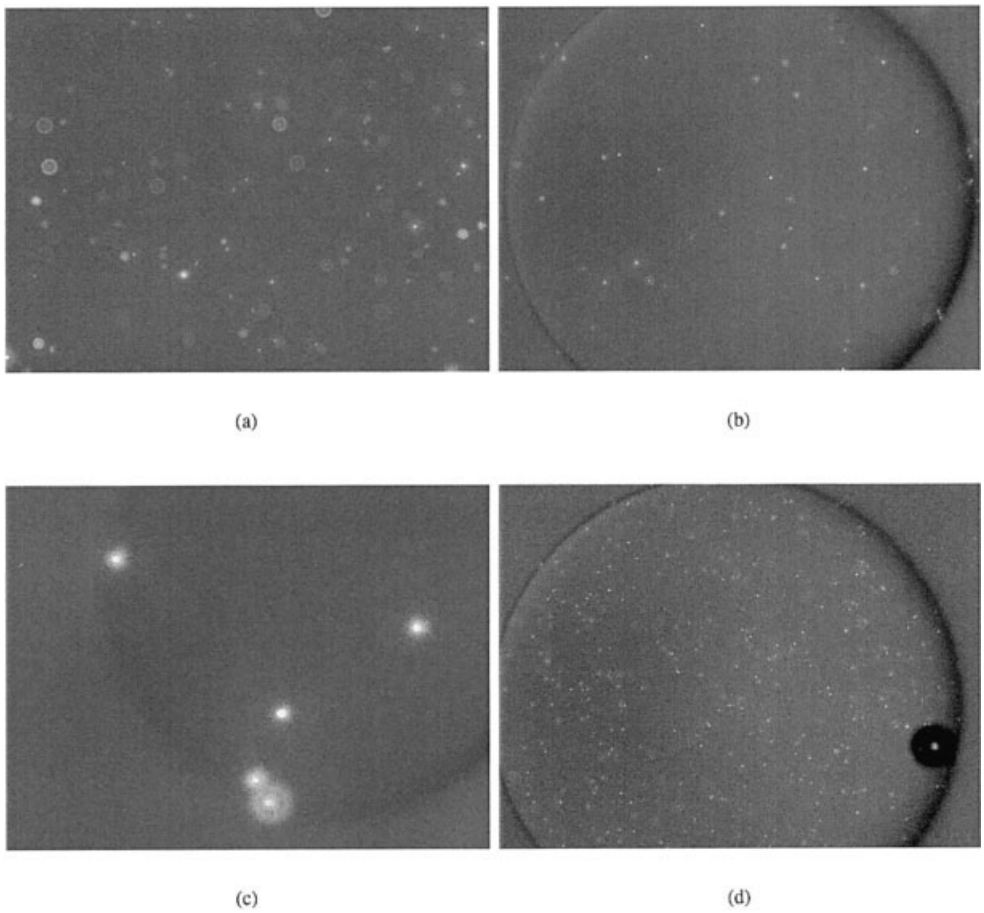

Fig. 1. Images of different microspheres in nanoliter wells filled with an aqueous solution of ethylene glycol in nanoliter wells (all displays log stretch). The image size is 1,334 × 1,024 pixels or 408 × 311 μm^2. **a:** Square well with pure water r = 95 nm. **b:** Round well with pure ethylene glycol r = 95 nm. **c:** 10% ethylene glycol r = 1,050 nm. **d:** 50% ethylene glycol, r = 55 nm. For the processing, a region of interest is manually selected such that the well borders are excluded.

$$D = \frac{k_B T}{6\pi\eta r}. \tag{1}$$

The denominator of eq.(1) is the Stokes friction coefficient $\mu = \upsilon/F$ of a sphere with radius r in a fluid with laminar velocity υ. The connection between the random motion of the microspheres and their average displacement is given by the diffusion equation

$$(\partial_t - D\Delta)\, f(x,t) = 0. \tag{2}$$

The expected position of a tracer particle after a time t is the initial position, but the variance of the observation is growing linearly with time

$$\langle x^2 \rangle = 2nDt, \tag{3}$$

where n is the number of *observed* spatial dimensions, i.e., each dimension contributes an equal $2Dt$. Here we have to keep in mind that the diffusion constant is independent of the dimensions observed and that the well is a 3D environment for the microbeads but we only observe 2D projections, thus measuring 2D distances. Therefore, for our evaluation we have to use $\langle x^2 \rangle = 4Dt$. The same result is obtained using the 3D relation and then applying the stereological correction factor for an ensemble $\langle x_{ob}^2 \rangle = \int_0^1 1 - z^2\, dz / \int_0^1 dz\, \langle x_{3D}^2 \rangle - 2/3 \cdot 6Dt = 4Dt$.

In our experiments, we want to measure the diffusion constant via observations of the variation of the squared displacement as a function of the radius of the microspheres and as a function of the viscosity of an aqueous solution of ethylene glycol. Finally we can compare the measurements with the theoretical values from eq.(1).

MATERIALS AND METHODS

We monitor the motion of the fluorescent microbeads under a microscope and extract their paths in time from the digital recordings. In Figure 1a–d we show typical images of wells filled with fluorescent microspheres. We used microspheres with radii of 55, 95, 280, 485, and 1,050 nm in solutions ranging from pure water to pure ethylene glycol ($C_2H_4(OH)_2$). For all experiments, we acquired between 150 and 360 time frames (100–600 s).

The experiments were performed with a Leica DM RXA confocal microscope, 20×/0.40 lens (in wide-field mode) with a Hamamatsu ORCA-ER C4742-95 CCD camera. The images were recorded with 12-bpp resolution and had a size of 1,344 × 1,024 pixels. The sampling density in the x- and y-direction was measured by placing a stage micrometer under the microscope: Δ_x =

Δ_y = 0.304 μm or 3.29 samples/μm. The microarray with wells of a size of 200 × 200 × 40 μm for closed wells and a diameter of 200 μm and a depth of 6 μm for the open wells was placed on a cooling stage that kept the temperature constant at T = 20°C (closed wells) and T = 25°C (open wells). Rhodamine-stained microspheres (Fluospheres, Molecular Probes, Leiden, The Netherlands, λ_{cx} = 580 nm and λ_{cm} = 605 nm) were used as tracer particles in all solutions. The microarrays were etched in silicon dioxide at DIMES (Delft Institute for Microelectronics and Submicron Technology).

For the closed wells, beads with radii in the range of r = 55–1,050 nm were used and viscosities in the range of η = 1.00–19.9 mPas. For the open wells, we used a single bead size of r = 280 nm and three different solutions with viscosities in the range of η = 1.5–14 mPas. The bead size and well depth were chosen to be identical to earlier experiments (Doel and Vliet, 2001; Rieger et al., 2003). We sealed the microarrays with a cover slip and then applied nail polish to prevent evaporation of the sample for the closed well experiments.

Diffusion Estimation and Tracking Algorithm

To estimate the displacement per tracer particle, we follow the individual particles over time and record their space-time position. In recorded images as depicted in Figure 1, there are many visible microspheres present (dependent on the radius of the spheres). Tracking of "blobs" is difficult if there is a high density of blobs. Below, we describe a practical and simple algorithm. For more sophisticated tracking methods, see for example Bergsma et al. (2001) Cavallo (2002), and Gerlich et al. (2001).

The first step in our algorithm is to segment the blobs from the background. For the larger microspheres, the signal-to-noise-ratio (SNR) is good as there is sufficient fluorescent material present. For smaller radii, the signal decreases rapidly because the total fluorescence goes with the third power of the radius and hence the (Poisson noise limited) SNR with $r^{3/2}$. Another complicating fact is the large depth-of-field. The well depth of 40 μm yields that many objects are severely defocused. Particularly the smaller objects become hard to detect since the apparent depth-of-field is dependent on the particle size (Ellenberger, 2000). The larger spheres can be detected far away from the focal plane where smaller spheres already "vanish." As a preprocessing step to enhance the blobs, we use a tophat filter $I - maxf(minf(I))$ (Verbeek et al., 1988). A manually selected threshold is applied to segment the objects. The objects in each time frame are labeled automatically. Starting from all detected objects in the first time frame, the nearest object in the following time frame is located (within a search radius of a few times the expected motion in this time interval). Due to the projection and finite resolution of the microscope, multiple "overlapping" objects may appear as a single blob. This in combination with other detection errors can produce ambiguous paths. With a post-processing step, only unique paths are extracted. Where two paths cross, we minimize the sum of the total path length. From theses paths, the diffusion constant is calculated from non-overlapping pairs at time points $\{i, i + \Delta t\}$, $\{i + \Delta t + 1, i + 2\Delta t + 1\}$, $\cdots$ of positions of an object. With this method, several independent estimates for D can be obtained from one tracer particle. A high number of pairs N is desirable to get a robust estimate for the diffusion constant.

As the microwells are limited in size, tracers, may strand at the well's sidewall. This would greatly mislead any diffusion calculation, therefore, only an inner region, several sphere radii from the border, is considered for the tracking. Microspheres that strand at the bottom or drift on the liquid surface are not detected at all, as the plane of focus is positioned in the middle of the well.

Sub-pixel estimation of the blob location is achieved by measuring the center of mass (intensity) inside a mask around the blob. See Localization accuracy and the MSD graph for a discussion of the effect that the localization error has on the mean square displacement (MSD) graph and the estimated diffusion constant.

It is to be expected that the outlined algorithm will not work equally well under all circumstances. The tracking will always choose the closest particle (which might not be the right one). The tracking will fail or choose the wrong particle more often for high diffusion constant and for high densities of tracer particles. In these cases, the algorithm is to be expected to produce a negative bias (underestimation of the true displacement). Evaluation of the algorithm on simulated Brownian motion of blobs in images has been done to verify this behavior.

Diffusion and Directed Motion in the Wells. The velocity of the evaporation flow in open wells is not constant over time during evaporation and is also dependent on the radial position of the tracer (Rieger et al., 2003). However, the velocity profile changes only slowly except in the last phase of the evaporation process, when the liquid meniscus approaches the bottom in the middle of the well. Therefore, we expect the motion in the early phase to be a superposition of diffusion with a constant velocity in the order of 0.1–0.3 μm/s (Rieger et al., 2003).

A superposition of directed motion with diffusion gives rise to the following additional term in eq. (3)

$$\langle x^2 \rangle = 2nDt + v^2t^2, \tag{4}$$

i.e., directed motion is characterized by a parabolic curve in the MSD graph. As a side note, restricted motion (due to confinement) is characterized by a curve that reaches a plateau value for larger lag times Δt.

MSD Graphs and the Estimation of Diffusion Constant. What is the best approach to estimate the diffusion constant and the MSD graph once the tracks (x, y, z, t positions of the particles) have been obtained? We suggest the following approach (let T be the total number of acquired time frames):

1. Compute the MSD graph from non-overlapping intervals.
2. Characterize the motion in an MSD graph up to max $\Delta t < T/2$, better $T/4$.
3. Compute the diffusion constant from $\Delta t = 1$ for pure diffusion and from a fit to $2nDt + v^2t^2$ for directed motion.

TABLE 1. Estimations of the diffusion constant $D_{theo} = k_B T / 6\pi\eta r$[1]

	% ethylene glycol in aqueous solution η[mPas] at T = 20°C					
	0	10	50	70	100	
r[nm]	1.00	1.27	3.8*	6.3*	19.9	D[μm²/s]
55			1.03			D_{theo}
			1.83 ± 0.19			D_{exp}
			1.23 ± 0.36			D_{fit}
			(124/2,459)			(n/N)
95	2.26	1.78	0.594	0.358	0.113	D_{theo}
	1.49 ± 0.083	1.30 ± 0.092	0.513 ± 0.026[2]	0.380 ± 0.027	0.100 ± 0.005	D_{exp}
	1.25 ± 0.021	1.47 ± 0.12	0.531 ± 0.058[2]	0.337 ± 0.0007	0.103 ± 0.016	D_{fit}
	(58/2,493)	(105/2,881)	(98/4,182)	(235/2,324)	(23/2,222)	(n/N)
280	0.766	0.603	0.201	0.122	0.0384	D_{theo}
	0.860 ± 0.083	0.612 ± 0.077	0.248 ± 0.036	0.128 ± 0.006	0.0491 ± 0.0024	D_{exp}
	0.712 ± 0.073[3]	0.730 ± 0.031	0.213 ± 0.010	0.126 ± 0.001	0.0495 ± 0.0007	D_{fit}
	(6/438)	(11/261)	(6/252)	(48/2,424)	(30/1,753)	(n/N)
485	0.442	0.348	0.116			D_{theo}
	0.410 ± 0.14	0.392 ± 0.06	0.137 ± 0.009			D_{exp}
	0.331 ± 0.17	0.463 ± 0.18[3]	0.116 ± 0.001			D_{fit}
	(3/42)	(3/162)	(18/1,591)			(n/N)
1050	0.204	0.160				D_{theo}
	0.153 ± 0.13	0.174 ± 0.051				D_{exp}
	0.447 ± 0.17	0.186 ± 0.005				D_{fit}
	(19/898)	(2/364)				(n/N)

[1]Measurements were performed with different combinations of microsphere radii and aqueous solutions of ethylene glycol. Viscosity values from Lide (1992), where values with * have been interpolated. 0% indicates pure water and 100% pure ethylene glycol. The mean value and the 95% confidence interval are shown for all measurements (D_{exp}) and the standard error for the fits to $4Dt$ (D_{fit}). n is the number of tracer particles extracted in the first time frame and N the number of position pairs used to compute $D = \langle x^2 \rangle / 4\Delta t \,|_{\Delta t = 1}$.
[2]The average of three repetitions of the same experiments.
[3]Here we fitted $4Dt + v^2t^2$ since during the experiment, there was a visible evaporation of induced liquid flow towards the borders of the well. See also the MSD graphs.

For the computation of the MSD graph, Saxton (1997, see the appendix) recommends to use averaging over dependent pairs, i.e., $\langle x^2 \rangle \,|_{\Delta t = i}$ is computed as a running average with size i instead of the average over independent pairs as shown above. The main reason is that a uniform sampling ensures equal weights to all data points. The differences in the two approaches are small for the MSD graph and the estimation of diffusion constant for small time lags. For large time lags, neither method gives reliable results. However, the application of the dependent average is error prone as people tend to show error-bars of one standard deviation computed from the average over correlated data and forget to apply the correct statistical treatment as in Qian et al. (1991). Furthermore, it is unclear in an application with binding effects if and how the statistics are influenced by the reaction kinetics.

In important earlier work by Qian et al. (1991) and Saxton (1997), a weighted fit of eq. (3) or eq. (4) to the MSD graph was suggested as the best approach to estimate the diffusion constant. The statistical weight of the ith point is its inverse variance from the formulas of Qian et al. (1991). This is the best method though more easily implemented in practice is to use the most reliable point only, i.e., $\Delta t = 1$, and disregard the rest as the weight is exponentially decreasing. For $\Delta t = 1$, the independent and dependent averages are equal. When using a weighted fit to the full MSD graph, diffusion constants obtained from averages over independent and dependent pairs are practically equal (Saxton, 1997).

Localization Accuracy and the MSD Graph. The accuracy of the estimated MSD depends on the accuracy with which a blob can be localized, as from these locations the (squared) distances are derived. Let σ_{loc} be the statistical uncertainty in the localization of x_0 and let it be Gaussian distributed; then we see that the estimated MSD has an offset dependent on the dimensionality n and σ_{loc}^2

$$\mathrm{MSD} \equiv \langle x^2 \rangle = \frac{1}{(2\pi\sigma_{loc}^2)^{n/2}} \int_{-\infty}^{\infty} dx\, (x - x_0)^2 e^{-(x - x_0)^2/2\sigma_{loc}^2} \quad (5)$$

$$= 2n\sigma_{loc}^2 + x_0^2 . \quad (6)$$

Next, we show that in the case of sealed wells this offset is negligible. If we assume very conservatively a localization uncertainty of $\sigma_{loc} = .5$ pixel, we have with a sampling density of 3.27 pixel/μm an offset of 0.0935 μm^2 in the MSD graph. In cases where there is a low localization accuracy (due to undersampling w.r.t. the Nyquist frequency) and/or little displacement (due to larger r or high η), this offset can be of interest and can influence the results when the offset is ignored.

RESULTS

In Table 1, we show the estimated diffusion constants for different aqueous solutions of ethylene glycol and different radii of the microspheres. We show the values computed for pairs separated by one time frame (the absolute time step varies slightly around 1 s). The number of initial tracers is given along with the number of pairs N used. We display the mean and the 95% confidence interval. Furthermore, we show the values obtained from a fit to the MSD graphs. In Figure 2, we show MSD graphs for a few of the experiments in closed wells. In Figure

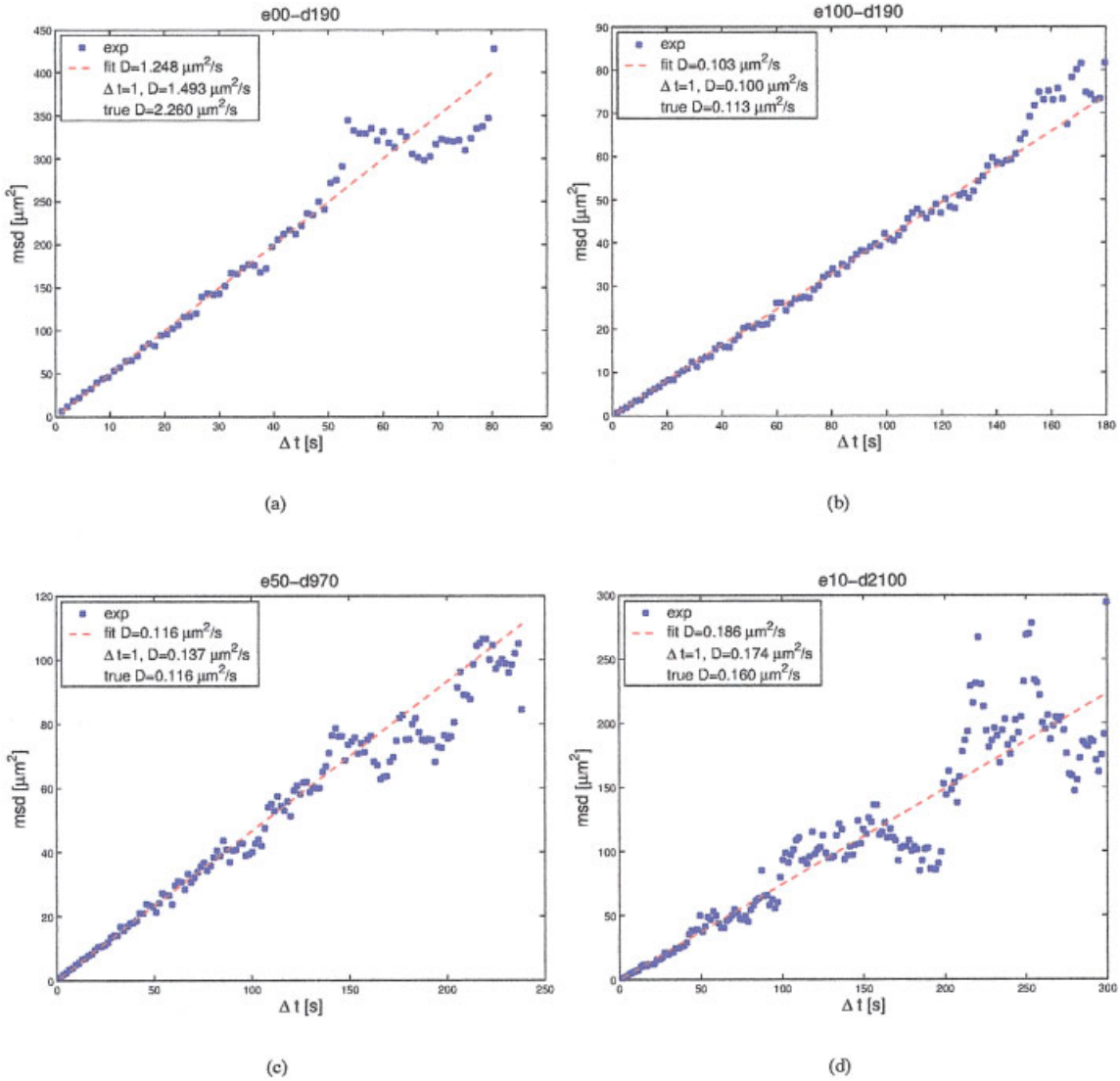

Fig. 2. Mean square displacement (MSD) graphs for selected experiments in closed wells. Indicated are the volume percentage of ethylene glycol and the diameter of the beads used in the experiment. [Color figure can be viewed in the online issue, which is available at www.interscience.wiley.com]

3a,b, we show MSD graphs for closed that leaked and for open wells in Figure 3c,d. The fits were done to diffusion motion only where a straight line was observed and to a combined diffusion and directed motion where a parabola was observed. A straight line clearly indicates diffusion behavior. A parabolic curve indicates an additional velocity component due to evaporation induced liquid flow in the open wells. In cases where we observe a parabolic curve for "sealed" wells, this shows that the sealing of the wells with a cover slip did not completely prevent evaporation. The velocity values obtained from the fits to the MSD graphs in Figure 3c,d of about 0.2 μm/s are in good agreement with values predicted and experimentally observed in early stages of the evaporation (Rieger et al., 2003).

The statistics are based on the estimation of an unknown mean from N independent normal distributed measurements (Student t-distribution). The estimated mean μ lies with a probability of $1 - \alpha$ within $\mu \pm \frac{s}{\sqrt{N}} t_{\alpha/2}(N-1)$, where $\alpha = 0.05$, N the number of pairs, s the measured standard deviation, and $t_{\alpha/2}(N-1)$ a tabulated value for the left- and right-sided percentile of the Student t-distribution (Bronstein et al., 1999). For our measurements we have $N \gtrsim 20$, $t_{\alpha/2}(N-1) \approx 2$.

In Figure 4, we plot the estimates for Dr (scale invariant) as a function of $1/\eta$ and for $D\eta$ (viscosity invariant) as a function of $1/r$. In general, the estimated values for the macroscopic diffusion constant are in agreement with the microscopic theory. We observe higher deviations from the theory for low viscosities and small marker sizes.

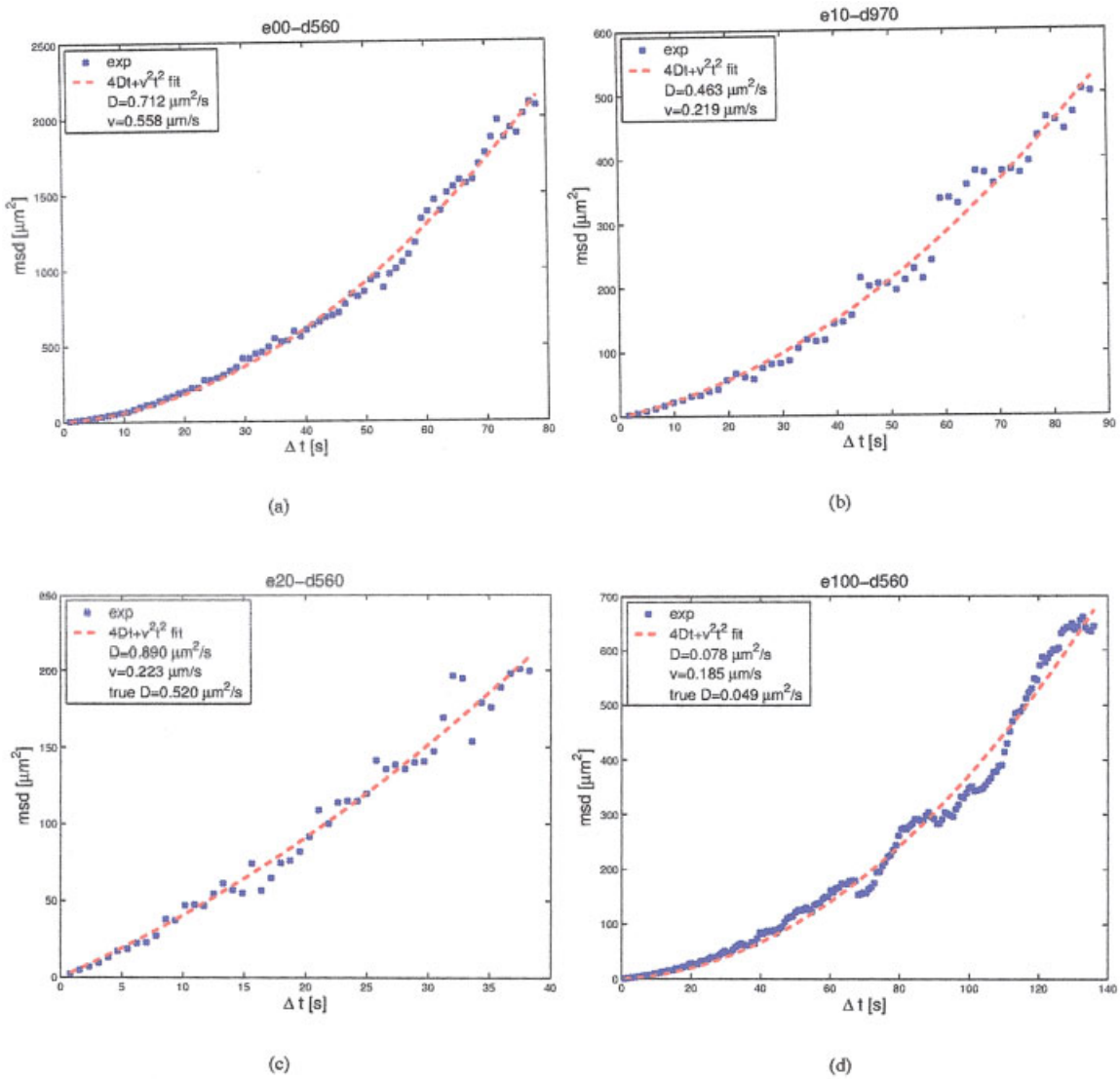

Fig. 3. Mean square displacement (MSD) graphs **(a,b)** for "closed" wells that showed a flow due to leakage and **(c,d)** for open wells. Indicated are the volume percentage of ethylene glycol and the diameter of the beads used in the experiment. [Color figure can be viewed in the online issue, which is available at www.interscience.wiley.com]

DISCUSSION

We showed that an absolute measurement of diffusion constants is possible with an image analysis technique. The presented experiment is in line with the one by the botanist Brown who noticed that pollen grains suspended in water jiggle when observed through the lens of a microscope (Brown, 1829). The prediction of the microscopic theory agrees with the macroscopic measurements.

The estimated diffusion constants are for both modalities (open and closed wells) in good agreement with theoretical predictions based on the Brownian motion and the flow model in the wells. We verify the degree of reliability of diffusion constant estimation not only from simulations but also from experiments with a known ground truth. The evaporation induced flow in the open microwells introduces a velocity component that is superimposed on the diffusion. The magnitude of this velocity and the diffusion constant can be reliably calculated also in these cases. For our algorithm, it is desirable to only have a few number of initial tracers resulting in a low density so that the tracking will not fail. To compensate for a lower number of pairs, the measurement time should be long, which enables more independent estimates from the same tracer particle.

ACKNOWLEDGMENTS

Bernd Rieger was supported by a TALENT fellowship from the Netherlands Organization for Scientific Research (NWO). The calculations were performed with the MATLAB toolbox DIPimage (Luengo Hendriks et al., 1999), which is freely available for academic usage.

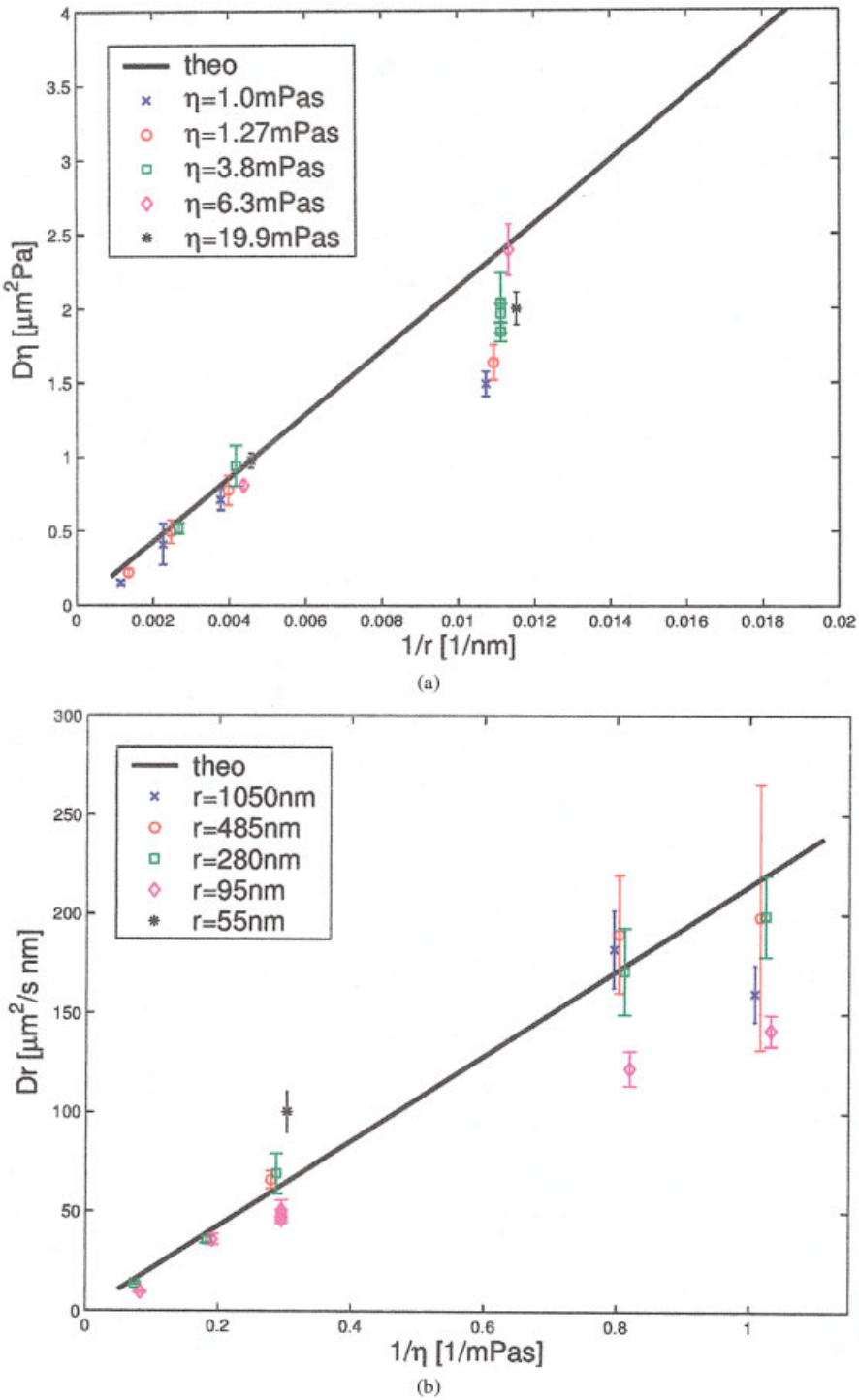

Fig. 4. Plots of the estimated diffusion constants of Table 1. **a:** $D\eta$ as a function of $1/r$. **b:** Dr as a function of $1/\eta$. [Color figure can be viewed in the online issue, which is available at www.interscience.wiley.com]

REFERENCES

Axelrod D, Koppel D, Schlesinger J, Elson E, Webb W. 1976. Mobility measurement by analysis of fluoresence photobleaching recovery kinetics. Biophys J 16:1055–1069.

Bergsma C, Streekstra G, Smeulders A, Manders E. 2001. Velocity estimation of spots in 3D confocal images sequences of living cells. Cytometry 43:261–272.

Bronstein I, Semendjajew K, Musiol G, Mühlig H. 1999. Taschenbuch der Mathematik, 4th ed. Thun Frankfurt (Main): Verlag Harri Deutsch.

Brown R. 1829. Additional remarks on active molecules. Philos Mag Ann Philos 6:161–166.

Cavallo A. 2002. Four dimensional particle tracking in biological dynamic processes. Ph.D. thesis, Ruprechts-Karls-Universität, Heidelberg, Germany.

Dietrich H, Knoll J, Doel Lvd, Dedem Gv, Daran-Lapujade P, Vliet Lv, Moerman R, Pronk J, Young I. 2004. Nanoarrays: a method for performing enzymatic assays. Anal Chem 76:4112–4117.

Doel Lvd, Vliet Lv. 2001. Temporal phase unwrapping algorithm for dynamic interference pattern analysis in interference-contrast microscopy. Appl Opt 40:4487–4500.

Einstein A. 1905. Über dic von der molekularkinetischen Thcoric der Wärme geforderte Bewegung von in ruhenden Flüssigkeiten suspendierten Teilchen. Annal Physik 17:549–560.
Ellenberger S. 2000. Influence of defocus on measurements in microscope images. Thesis. Technische Universiteit Delft. Delft, The Netherlands.
Gerlich D, Beaudouin J, Gebhard M, Ellenberg J, Eils R. 2001. Four-dimensional imaging and quantitative reconstruction to analyse complex spatiotemporal processes in living cells. Nature Cell Biol 9:852–855.
Kubitscheck U, Kückmann O, Kues T, Peters R. 2000. Imaging and tracking of single GFP molecules in solution. Biophys J 78:2170–2179.
Kues T, Kubitscheck U. 2002. Single molecule motion perpendicular to the focal plane of a microscope: application to splicing factor dynamics within the cell nucleus. Single Molecule 3:218–224.
Kutsumi A, Sako Y, Yamamoto M. 1993. Confined lateral diffusion of membrane receptors as studied by single particle trackin (Nanovid Microscopy). Biophys J 65:2021–2040.
Lide D, (editor). 1992. Handbook of Chemistry and Physics, 82nd ed. Boca Raton: CRC Press.
Luengo Hendriks C, Rieger B, Ginkel Mv, Kempen Gv, Vliet Lv. 1999. DIPimage: a scientific image processing toolbox for MATLAB. Delft University of Technology, http://www.ph.tn.tudelft.nl/DIPlib.
Qian H, Sheetz M, Elson E. 1991. Single particle tracking: analysis of diffusion flow in two-dimensional systems. Biophys J 60:910–921.
Rieger B, Doel Lvd, Vliet Lv. 2003. Ring formation in nanoliter cups: quantitative measurements of flow in micromachined wells. Phys Rev E 68:036312.
Saxton M. 1997. Single-particle tracking: the distribution of diffusion coefficients. Biophys J 72:1744–1753.
Sprague B, Pego R, Stavreva D, McNally J. 2004. Analysis of binding reactions by fluorescence recovery after photobleaching. Biophys J 86:3473–3495.
Valeur B. 2002. Molecular fluorescence. Weinheim: Wiley-VCH.
Verbeek P, Vrooman H, Vliet Lv. 1988. Low-level image processing by Max-Min filters. Signal Process 15:249–258.
Young I, Moerman R, Doel Lvd, Iordanov V, Kroon A, Dietrich H, Dedem Gv, Bossche A, Gray B, Sarro L, Verbeek P, Vliet Lv. 2003. Monitoring enzymatic reactions in nanolitre wells. J Microsc 212:254–263.